



The utility of forest attribute maps for automated Avalanche Terrain Exposure Scale (ATES) modelling

Johannes Schumacher, Håvard Toft, J. Paul McLean, Marius Hauglin, Rasmus Astrup & Johannes Breidenbach

To cite this article: Johannes Schumacher, Håvard Toft, J. Paul McLean, Marius Hauglin, Rasmus Astrup & Johannes Breidenbach (2022): The utility of forest attribute maps for automated Avalanche Terrain Exposure Scale (ATES) modelling, Scandinavian Journal of Forest Research, DOI: [10.1080/02827581.2022.2096921](https://doi.org/10.1080/02827581.2022.2096921)

To link to this article: <https://doi.org/10.1080/02827581.2022.2096921>



Published online: 11 Jul 2022.



Submit your article to this journal [↗](#)








View related articles [↗](#)



View Crossmark data [↗](#)



The utility of forest attribute maps for automated Avalanche Terrain Exposure Scale (ATES) modelling

Johannes Schumacher ^a, Håvard Toft ^{b,c}, J. Paul McLean^a, Marius Hauglin ^a, Rasmus Astrup ^a and Johannes Breidenbach ^a

^aNorwegian Institute of Bioeconomy Research (NIBIO), Ås, Norway; ^bNorwegian Water Resources and Energy Directorate (NVE), Oslo, Norway;

^cCenter for Avalanche Research and Education, UiT The Arctic University of Norway, Tromsø, Norway

ABSTRACT

The number of people affected by snow avalanches during recreational activities has increased over the recent years. An instrument to reduce these numbers are improved terrain classification systems. One such system is the Avalanche Terrain Exposure Scale (ATES). Forests can provide some protection from avalanches, and information on forest attributes can be incorporated into avalanche hazard models such as the automated ATES model (AutoATES). The objectives of this study were to (i) map forest stem density and canopy-cover based on National Forest Inventory and remote sensing data and, (ii) use these forest attributes as input to the AutoATES model. We predicted stem density and directly calculated canopy-cover in a 20 Mha study area in Norway. The forest attributes were mapped for 16 m × 16 m pixels, which were used as input for the AutoATES model. The uncertainties of the stem number and canopy-cover maps were 30% and 31%, respectively. The overall classification accuracy of 52 ski-touring routes in Western Norway with a total length of 282 km increased from 55% in the model without forest information to 67% when utilizing canopy cover. The F1 score for the three predicted ATES classes improved by 31%, 9%, and 6%.

ARTICLE HISTORY

Received 3 March 2022

Accepted 28 June 2022

KEYWORDS

Airborne laser scanning;
National Forest Inventory;
SR16; disaster risk reduction;
nature-based solutions

Introduction

Snow avalanches cause on average six fatalities per year in Norway (NGI 2022; Varsom 2022); these deaths and other injuries are primarily associated with recreation. Likely due to the increased use of the outdoors, the number of people affected by avalanches has increased remarkably in the recent years (Varsom 2022). Considerable resources have therefore been invested to reduce the number of casualties. Avalanche terrain classification maps to assist route finding are believed to be an important tool in this context. Forest cover can alter avalanche behaviour by reducing the snow-pack through canopy interception (Bebi et al. 2001) and, albeit to a lesser extent, by increasing friction on prone slopes through the mechanism of the physical barriers of tree stems (Teich et al. 2014). On the other hand, large avalanches that release far above the tree line are only to a small degree affected by forests (Teich et al. 2012) and tree debris in those avalanches can increase the likelihood of trauma for people affected by the avalanche. Snow interception is largely dependent on tree species, because of the different morphology of tree crowns, and the size and number of trees in a given area, which are the factors that will collectively determine canopy cover and gaps. These parameters can potentially be derived from remote sensing in a way that is suited to avalanche simulation because they are spatially explicit (Brožová et al. 2020). Maps of such forest attributes allow for monitoring of forest development and,

subsequently, for adequate and effective forest management towards an optimized avalanche protection function to reduce avalanche hazards (Brang et al. 2006). This is especially crucial under the challenge of climate change that requires us to adapt forests to changing growing conditions to maintain healthy and resilient forests that can fulfil their functions. Moreover, once avalanche terrain zones are mapped, forest management measures could be used to reduce avalanche hazard, for example by avoiding clear cuts.

Two types of avalanche hazard modelling can be distinguished: (i) terrain classification for recreational trip planning and (ii) hazard mapping for land use planning. The main difference is that much more frequent avalanche return periods are acceptable for recreational trip planning where local conditions can flexibly be considered as opposed to the case of hazard mapping for land use planning. Here, we focus on avalanche terrain classification for recreational trip planning. Worldwide, various avalanche terrain classification maps have been developed for recreationalists using different avalanche classification schemes (Barbolini et al. 2011; Schmudlach and Köhler 2016; Harvey et al. 2018; Larsen et al. 2020b). In Norway, the most used classification of avalanche terrain is the Avalanche Terrain Exposure Scale (ATES, Statham et al. 2006). The classification scheme divides avalanche terrain into simple (class 1), challenging (class 2) and complex (class 3) terrain.

Originally, the ATES classification scheme was developed to provide an overall classification of an entire route based

on the overall exposure likely to be encountered. Recent advances including modern cartographic techniques have made it more common to develop spatial maps. Making ATES maps, Delparte (2008) found that slope angle and stem density were the two most important factors when classifying avalanche terrain with the ATES model. Campbell and Gould (2013) developed a specific model for spatial ATES including parameters for slope angle and forest density. Building on the proposed model for spatial ATES mapping, Larsen et al. (2020a, 2020b) developed an automated ATES algorithm (AutoATES) for nationwide maps in Norway. The algorithm comprises the components potential release area (PRA) (Veitinger et al. 2016; Sharp et al. 2018) and a gravitational mass flow simulation (FlowPy) (D'Amboise et al. 2021). However, due to limits in the spatial resolution and area coverage of forest data, this version of the algorithm was only developed for non-forested terrain so far. The Auto-ATES map is consequentially likely to be inaccurate below the treeline. While most recreational accidents associated with avalanches happen above the treeline, Norway is not a country with particularly high mountains and the fjordic landscape means that a considerable amount of avalanche prone terrain is found below the treeline. Therefore, the inclusion of forest attributes in terrain exposure classification is important. Consequentially, in this study, we analyse the possibility to integrate high spatial resolution data on forests into the spatially explicit classification of avalanche exposure (Auto-ATES-Forest).

The relationship between forest attributes and remote-sensing data can be quantified via regression models, where the response (a forest attribute) is explained by predictors (remotely sensed variables). Such models are usually established using ground reference data from field plots with known locations and remote-sensing data extracted for the same locations. This is commonly known as the area-based approach (Næsset 2002). In Norway, the National Forest Inventory (NFI) collects extensive information about forest attributes in sample plots with a size of 250 m² (Breidenbach et al. 2020a), which can serve as a ground reference for remote-sensing data to establish regression models predicting these forest attributes. Once established, these models can be applied to areas beyond field-inventory plots, to obtain prediction maps for the attributes of interest. These predictions are particularly useful to support operational forest management (e.g. reviewed by Brososke et al. 2014), but can also be used as input for other purposes such as terrain classification for avalanche hazard maps. To achieve this mapping of forest attributes, the entire area is gridded into area units of the same size as used for model fitting on NFI plots, and the same remotely sensed variables are extracted for each unit. Following this approach, various forest attributes were modelled and mapped for the Norwegian forest resource map SR16 (Astrup et al. 2019; Hauglin et al. 2021), which is a national map at a spatial resolution of 16 m × 16 m that is freely available (NIBIO 2022).

The necessary forest attributes for the AutoATES-Forest avalanche terrain classification model in Norway are canopy cover or stem density. Canopy cover is defined as the proportion of the forest floor that is obscured by tree crowns.

Consequentially, airborne laser scanning (ALS) is the ideal way in which to assess this variable directly for example from a surface model or as the proportion of first returns above a specified height threshold (Korhonen et al. 2011). On the other hand, stem density is more challenging to obtain from wide-area coverage ALS because the lasers do not penetrate the canopy with sufficient spatial resolution to directly observe the stems. Therefore, the aforementioned relationships need to be quantified. Previous studies have attempted to do this in comparable forest types (Næsset and Bjerknes 2001; Lindberg et al. 2010; Ene et al. 2012; Lindberg and Hollaus 2012; Eysn et al. 2015). In general, the model errors are quite high compared to volume or tree height and these increase with increasing complexity of the forest in terms of species and age structure. As none of the currently available models are applicable to the national level in Norway, it was an important facilitating aim in the current study to develop those models.

Our objectives were twofold: (I) to describe empirical models linking stem density (number of trees per ha) observed at NFI sample plots to ALS metrics that are used to map this forest attribute in a fine resolution of 16 m × 16 m and to map canopy cover obtained directly from ALS data; and (II) to demonstrate and assess the inclusion of these in the Auto-ATES-Forest avalanche terrain classification model for recreational activities. For the latter, we use expert-classified skitouring routes in Western Norway as a reference. To the best of our knowledge, this is the first study that documents the use of high-resolution forest maps for the improvement of avalanche maps for recreational purposes.

Material and methods

Study areas

In this study, we referred to two different areas for the different analysis levels: modelling forest attributes (large part of Norway), and modelling avalanche terrain classes for recreational activities (backcountry skiing area Romsdalen).

For modelling forest attributes with field reference data and auxiliary remote-sensing data, we used NFI data from a large part of the country covering 21.5 Mha (66% of the Norwegian mainland), located in Norway between latitudes 58.0° and 69.5° N. This spatial extent was determined by the availability of ALS data (Figure 1). Within the study area, forest growing conditions vary considerably with latitude and elevation. The natural tree line is at around 1100 m asl in southern Norway and around 130 m asl in the north. Depending on these factors, climate zones range roughly from subarctic in the north and east, oceanic at the west coast, and continental in the south-east. The tree species are primarily Norway spruce (*Picea abies*) and Scots pine (*Pinus sylvestris*). These make up the majority of above-ground biomass and standing volume. Birch (*Betula pendula* and *B. pubescens*) is the most abundant species in terms of tree number and mainly occurs as early succession following disturbance (including timber harvests) or in high elevation or latitude forests (Breidenbach et al. 2020a). In this study, the term broadleaved is used to represent what are mostly birch forests.

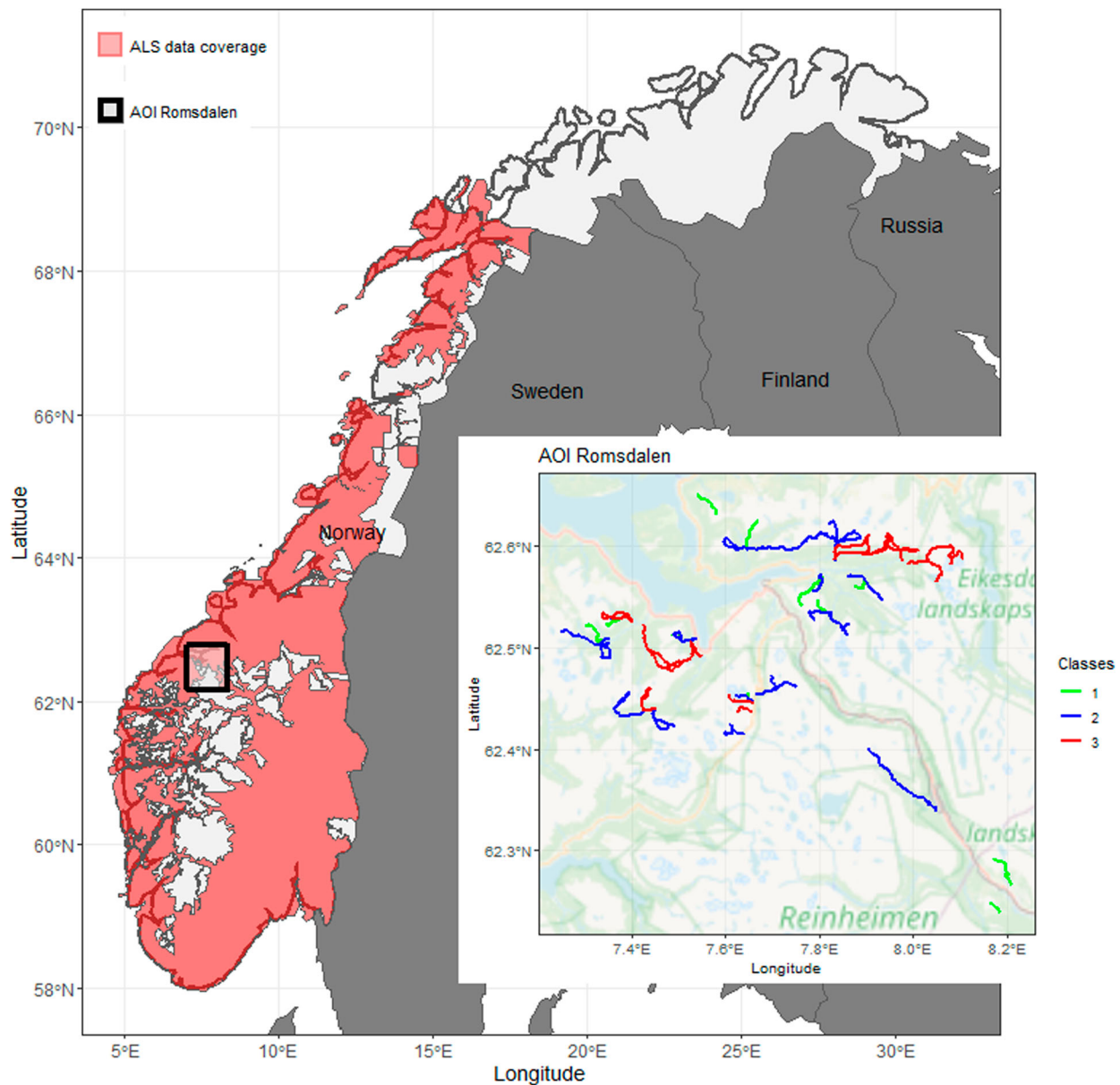


Figure 1. Study area with airborne laser scanner (ALS) data coverage used for modelling forest characteristics, and Romsdalen area including ski-touring routes through mountainous terrain. The terrain and touring routes are classified according to the ATEs classification scheme with classes 1 – simple (green), 2 – challenging (blue), 3 – complex (red).

For assessing the effect of forest towards improved avalanche terrain models for recreational activities we used the area of Romsdalen (Figure 1). This region is a popular destination for ski-touring attracting national and international visitors. Within this area, we focused on forested areas on slopes that were relevant for avalanche terrain mapping along 52 documented ski-touring routes (see section Reference data generation: avalanche terrain classification for routes). The study area has an area of 3200 km² and the mountains reach from sea level and up to 1784 m above sea level.

Mapping forest attributes

To map the forest attribute stem density, we developed a mixed-modelling regression between this attribute (our response variable) and independent predictor variables

calculated from remote-sensing data. We used field-measured stem density from the Norwegian NFI (Breidenbach et al. 2020a) as the response variable, and remote-sensing data from airborne laser scanning (ALS) and Sentinel-2 satellite images (S2) as independent predictor variables (sections Modelling and mapping tree density and Mapping canopy cover). The attribute canopy cover was obtained from the ALS data directly and compared to and visually assessed canopy cover in the NFI.

Data

National Forest Inventory (NFI) data. We used the permanent sample plots of the Norwegian NFI as reference data (Breidenbach et al. 2020a). In the study area, the NFI is based on a systematic grid of 3 km × 3 km in the lowland region and 3 km × 9 km in the low-productive, birch-

Table 1. Summary statistics of the Norwegian national forest inventory (NFI) data used for modelling in this study.

	Height ^a (m)	Volume ^b (m ³)	Stem density ^c	Canopy cover (%)
Overall				
Min	4.9	5.2	40	0
Max	34.1	1144.7	2840	99.0
Mean	15.2	208.9	860	68.5
STD	4.4	152.2	463	23.3
Spruce				
Min	5.7	7.6	40	3.0
Max	34.1	1144.7	2840	99.0
Mean	17.0	277.1	1030	75.8
STD	4.4	172.2	451	19.5
Pine				
Min	7.2	12.7	40	5.0
Max	28.3	693.7	2560	99.0
Mean	14.8	176.2	652	64.4
STD	3.5	106.2	370	22.0
Broadleaved trees				
Min	4.9	5.2	40	0.0
Max	26.4	400.7	2760	99.0
Mean	11.3	101.7	845	60.2
STD	3.5	70.9	485	28.1

^aBasal area BA weighted mean tree height.^bVolume with bark.^cNumber of trees ≥ 8 cm diameter at breast height (dbh) per ha.

dominated mountain region. For trees with a diameter at breast height ≥ 5 cm (dbh, 1.3 m above ground), parameters are measured on circular plots with a size of 250 m².

For modelling stem density, we used NFI plots located in stands dominated by spruce, pine, and broadleaved trees (defined as plots with $\geq 75\%$ timber volume of each tree species, respectively). From these plots, we only selected NFI plots in one-layered forests for stem density modelling, resulting in 1351 spruce, 1064 pine, and 535 broadleaved dominated plots that were used for modelling stem density (Table 1).

Canopy cover is visually assessed only for unproductive forest and other wooded land in the NFI (Viken 2021, p. 69) and, therefore, the number of plots used for the analysis of the ALS-based canopy cover measurement was 247, 205, and 112 for spruce, pine, and broadleaved forest, respectively.

Remote-sensing data. ALS data were acquired during several measurement campaigns for the study area between 2010 and 2019 with a density of 2–5 pulses per m². A high-resolution digital terrain model (DTM, 1 m \times 1 m pixel size) was produced from the last-return data by the Norwegian Mapping Authority (Kartverket 2019). The ALS point cloud was height-normalized by subtracting the DTM elevation from the corresponding point cloud elevation using bi-directional interpolation. The height-normalized point cloud was used to calculate various descriptive metrics for each NFI plot based on first returns, first returns above 2 m height above ground, and last returns. The metrics included mean, variance, coefficients of variation, kurtosis and skewness of ALS return heights, 10th, 25th, 50th, 75th, 90th, and 95th height percentiles, and ALS return density metrics for 10 individual height slices (d0–d9). A canopy coverage metric was calculated as the percentage of first returns above 2 m (pctab2f). The DTM was resampled to 16 m \times 16 m, such that the cell size corresponded

approximately to the area covered by an NFI plot (250 m²). From the DTM, terrain slope was computed as a raster with a cell size of 16 m \times 16 m. S2 bottom of atmosphere reflectance images acquired between 30 June and 31 July 2018 were mosaiced using the bands B2 (blue), B3 (green), B4 (red), B5 (red edge), B6, B7, B8 and B8A (near infrared), B11 and B12 (short wave infrared), measuring reflectance in the visible, NIR and SWIR spectrum (Drusch et al. 2012). The normalized difference vegetation index (NDVI) was calculated as band 8 minus band 4 divided by band 8 plus band 4 and tested as a predictor in the prediction models.

Modelling and mapping tree density

In the Norwegian forest resource mapping project SR16 (Astrup et al. 2019; Hauglin et al. 2021) linear-mixed regression models were developed to estimate various forest properties. These models have the structure:

$$y = \mathbf{X}\beta + \mathbf{Z}u + \epsilon, \text{ with } u \sim N(0, \mathbf{G}) \text{ and } \epsilon \sim N(0, \mathbf{R}) \quad (1)$$

where y is the dependent response variable, \mathbf{X} and \mathbf{Z} are the design matrices for fixed and random effects, respectively, β are the fixed effects parameters, u is a vector of random effects, and \mathbf{G} and \mathbf{R} are the covariance matrices for random effects and residual errors, respectively. We used the nlme package (Pinheiro et al. 2020) in the statistics software R (R Core Team 2020) to estimate the model parameters. A starting model was stepwise reduced by forward and backward selection of predictors based on Akaike Information Criterion as a stopping rule (stepAIC function in R (Venables and Ripley 2002)) and was further reduced by backward selection based on p -values ($p < .05$). We used the information on ALS project acquisition as a random effect on the intercept in the models to account for differences in ALS data collection between the different projects. Among others, we used the predicted coefficient of determination, R^2 , for model assessment

$$\text{Predicted } R^2 = 1 - \frac{\sum_{i=1}^n (y_i - \hat{y}_i)^2}{\sum_{i=1}^n (y_i - \bar{y})^2} \quad (2)$$

where y_i and \hat{y}_i are observed and predicted values in unit i and the number of units is denoted by n .

We used the approach described above and the model structure in Equation (1) to fit linear-mixed-effects models predicting stem density (for trees ≥ 8 cm dbh) for three tree species of interest. Area-wide predictions of the forest attributes were made by applying the developed models to 16 m \times 16 m pixels, which is similar to the area of the NFI plots used during model fitting. A tree species map (Breidenbach et al. 2020b) was used to apply the corresponding tree species-specific model.

Mapping canopy cover

Canopy cover was calculated from the ALS data directly by analysing the spatial distribution of laser echoes with above-ground heights ≥ 5 m. The normalized laser point cloud of each 16 m \times 16 m pixel was divided into 64 voxels of size $2 \times 2 \times h$ m³, where h is the vertical distance from 5 m above ground to the maximum above-ground echo

Table 2. ATES Public Communication Model (v1.04) (Statham et al. 2006), and summary of the 52 documented ski-touring routes in Romsdalen used in this study.

Description	Class	Terrain criteria for avalanche exposure (relevant excerpt)	# Routes	Total length (km)
Simple	1	Exposure to low angle or primarily forested terrain. Some forest openings may involve the runout zones of infrequent avalanches. Many options to reduce or eliminate exposure	12	43
Challenging	2	Exposure to well defined avalanche paths, starting zones or terrain traps; options exist to reduce or eliminate exposure with careful route finding	26	131
Complex	3	Exposure to multiple overlapping avalanche paths or large expanses of steep, open terrain; multiple avalanche starting zones and terrain traps below; minimal options to reduce exposure	14	108

height. Each voxel was thus defined by a $2 \times 2 \text{ m}^2$ base at 5 m above ground and extended upwards to the height of the highest echo, i.e. h . Note that this means that the shape of the voxels where in most cases not cubical, but typically were higher than the 2 m sides of the base and that forests smaller than 5 m height will have a crown cover of 0. The proportion of non-empty voxels was used as a representation for canopy cover in the $16 \text{ m} \times 16 \text{ m}$ pixel, with non-empty voxels being voxels containing at least one laser echo. Canopy cover was then compared to field-based estimates of canopy cover at NFI plots.

Avalanche terrain classification maps for recreational activities

Reference data generation: avalanche terrain classification for routes

As a basis for comparison in the case study area, we used the available ATES classification of ski-touring routes by local avalanche experts in Romsdalen, Norway. The dataset consists of 52 routes with a total length of 282 km (Figure 1, Table 2) that were manually mapped by local avalanche experts of the Norwegian Water Resources and Energy Directorate (NVE) in 2018 (Larsen et al. 2020b). NVE is the government authority for avalanche hazard mapping in Norway. The work was done using the ATES v1.04 defined by Statham et al. (2006) presented in Table 2. Methods used included: a GIS web tool, visual interpretation of aerial imagery, local expertise, and field

surveys. Each route is classified according to eleven different avalanche terrain factors and classified as either simple, challenging, or complex terrain. If the route is within the challenging or complex definition of slope angle for a short section of the trip, the whole trip will be classified as challenging or complex.

The AutoATES model

To investigate the effect of forest data on ATES maps for recreational activities, we used the AutoATES algorithms developed by Larsen et al. (2020a, 2020b). We examined the impact of using either canopy cover or stem density and compared it to AutoATES with no forest data as input as per Larsen et al. (2020a, 2020b). AutoATES is an automated algorithm that is made to create spatial ATES maps using a DEM and optional forest data as input. In the present study, a DEM based on ALS data was used (Kartverket 2019).

The full methodology of the AutoATES model is described in detail in Larsen et al. (2020b), and it will therefore only be briefly presented here. The first step of the algorithm is to calculate the potential release areas (PRA) using the algorithm developed by Veitinger et al. (2016). Using a fuzzy operator, they combine the input variables slope angle, terrain roughness, and wind shelter using a Cauchy membership value (Jang et al. 1997). Sharp et al. (2018) modified the algorithm to also include stem density. Previously, stem density has not been available in high resolution in Norway. Cauchy membership values must be defined for each input variable:

$$\mu(x) = \frac{1}{1 + \left(\frac{x - c}{a}\right)^{2b}} \quad (3)$$

where $\mu(x)$ is the Cauchy membership value, x is an input variable, and a , b , and c are parameters which control the weight of each input variable. We use the parameter values suggested by Sharp et al. (2018) for slope angle, roughness, wind shelter, and stem density. This means that the forest attribute is one of four input parameters in the PRA algorithm. There are currently no parameter values documented for canopy cover, therefore we set the values as given in Table 3. A fuzzy operator is used to generate the final PRA values as a result of the four Cauchy membership values (Table 3) (Veitinger et al. 2016; Sharp et al. 2018).

In a second step, which is independent of forest attributes, a runout model is used to calculate areas downslope of the PRAs that could be affected by an avalanche. FlowPy (D'Amboise et al. 2021) is used for modelling runout, which is a flow model that is limited by the angle of reach, i.e. the angle from the top of the PRA to the lowermost point of the avalanche path (Larsen et al. 2020b). The AutoATES algorithm is controlled by parameters for slope angle threshold (SAT), cell count (CC), angle of reach (AAT), and PRA threshold (PRA THD) (Table 4). Using these parameters, the model outputs a preliminary layer with the categorical classes simple, challenging, and complex terrain.

In a third step, to account for forest attributes in the runout zone, the forest map information of each pixel is split into four categories ranging from open to dense (Table 5). Using a set of map algebra equations on each of these categories, the ATES classifications are either kept the same, or

Table 3. The parameters used to calculate the Cauchy membership values (Equation (3)) in the PRA model.

Parameter:	a	b	c
Slope angle (Sharp et al. 2018)	7	2	38
Roughness (Sharp et al. 2018)	0.01	5	-0.007
Wind shelter (Sharp et al. 2018)	2	3	2
Stem density (Sharp et al. 2018)	350	2.5	-150
Canopy cover	240	25	-200

Table 4. The input parameters used for AutoATES (Larsen et al. 2020b). The parameters were used in models that included either no forest data, stem density, or canopy cover.

Parameter:	AAT1	AAT2	AAT3	CC1	CC2	SAT1	SAT2	SAT3	SAT4	PRA THD
Value:	20°	25°	31°	50	250	15°	25°	31°	37°	0.15

altered to a lower ATES class value (Larsen et al. 2020b). For example, if the initial ATES class is 3 (complex) but the forest is dense, the final ATES classification is reduced to class 2 (challenging).

To compare the AutoATES classification with the manual ATES classification for skiing routes, the values of the AutoATES map were extracted every 10 m along the length of the route. The 95th percentile of the extracted AutoATES map predictions was used to assign one predicted class per route.

Evaluation criteria

We used the evaluation criteria Root Mean Squared Error (RMSE), and RMSE% to evaluate the modelled forest attribute stem density and the calculated canopy cover (Equations (4) and (5)).

$$\text{RMSE} = \sqrt{\frac{1}{n} \sum_{i=1}^n (y_i - \hat{y}_i)^2} \quad (4)$$

$$\text{RMSE\%} = 100 \times \frac{\text{RMSE}}{\frac{1}{n} \sum_{i=1}^n (y_i)} \quad (5)$$

where y_i and \hat{y}_i are observed by field inventory (NFI) and predicted values in unit i . The number of units in data is denoted by n .

To evaluate the overall route classification, we used overall accuracy (OA), and to evaluate each class separately we used producers' accuracy (PA – the proportion of correctly classified observed values), users' accuracy (UA – the proportion of correctly classified predicted values), and F1 score (combines UA and PA into one metric) according to (Congalton and Green 2008).

$$\text{OA} = \frac{\sum \text{True positives}}{\text{Total number of observations}} \quad (6)$$

$$\text{PA} = \frac{\text{True positive}}{\text{True positive} + \text{False negative}} \quad (7)$$

$$\text{UA} = \frac{\text{True positive}}{\text{True positive} + \text{False positive}} \quad (8)$$

$$\text{F1} = 2 \times \frac{\text{PA} \times \text{UA}}{\text{PA} + \text{UA}} \quad (9)$$

All accuracy metrics were derived from the length of routes in the confusion matrix that is also provided. In the confusion

matrix, predicted and observed ATES classes for routes are tabulated which gives the full overview of the classification result in a condensed manner.

Results

Forest attribute maps

We modelled stem density using linear-mixed-effects models, and directly calculated canopy cover from ALS data for spruce, pine, and broadleaved forests (Figure 2). The fit statistics associated with the linear-mixed models for stem density showed that the results for spruce were the most accurate in terms of leave-one-out cross-validated $\text{RMSE}_{\text{cv}}\%$ (Table 6). The significant predictors were similar for the spruce and pine models. Both models contained the 75th percentile of first ALS returns (h75f), and its squared version (h75fsq), the percentage of first ALS returns above 2 m height (pctab2f), and its squared version (pctab2fsq), the interactions between h75f and pctab2f, and between h75fsq and pctab2fsq, the normalized difference vegetation index (NDVI), and terrain slope. For the spruce model, one additional first return density metric d6f was included, and for the pine model, the first return density metric d4f was included. The model for broadleaved forests only included the predictors h75fsq, pctab2fsq, and d6f. Model details and variance components of the stem density models are presented in Appendix in Tables A1 and A2.

The R^2 of the stem density models was 0.59, 0.56, 0.68, and 0.62 for spruce, pine, broadleaved, and all forest, respectively. The Pearson correlation between canopy cover directly obtained from the ALS data and canopy cover assessed at NFI plots was 0.58, 0.67, 0.62, and 0.64 for spruce, pine, broadleaved, and all forest, respectively (Figure 2, Table 6).

The two plots in broadleaved forest that have zero predicted canopy cover (Figure 2, bottom right) are due to low tree heights. Since we only used ALS returns above 5 m height, canopy cover predictions are less accurate in low forest.

Assessment of avalanche terrain maps for recreational activities

Overall, including forest attributes in the AutoATES model improved terrain and, thereby, route classifications with regard to avalanche hazard (Figure 3). Using the 95th percentile of predicted values to assign one class per route, AutoATES-Forest classifications showed a considerable improvement compared to AutoATES without forest attributes (Table 7).

Overall accuracies weighted by route lengths increased from 0.55 for AutoATES to 0.67 for AutoATES-Forest using canopy cover and to 0.63 for AutoATES-Forest using stem

Table 5. The parameters used to account for forest density in the avalanche runoff.

Category	Open	Sparse	Average	Dense
Stem density (n/ha)	0–100	100–250	250–500	>500
Canopy cover (%)	0–10	10–25	25–65	65–100

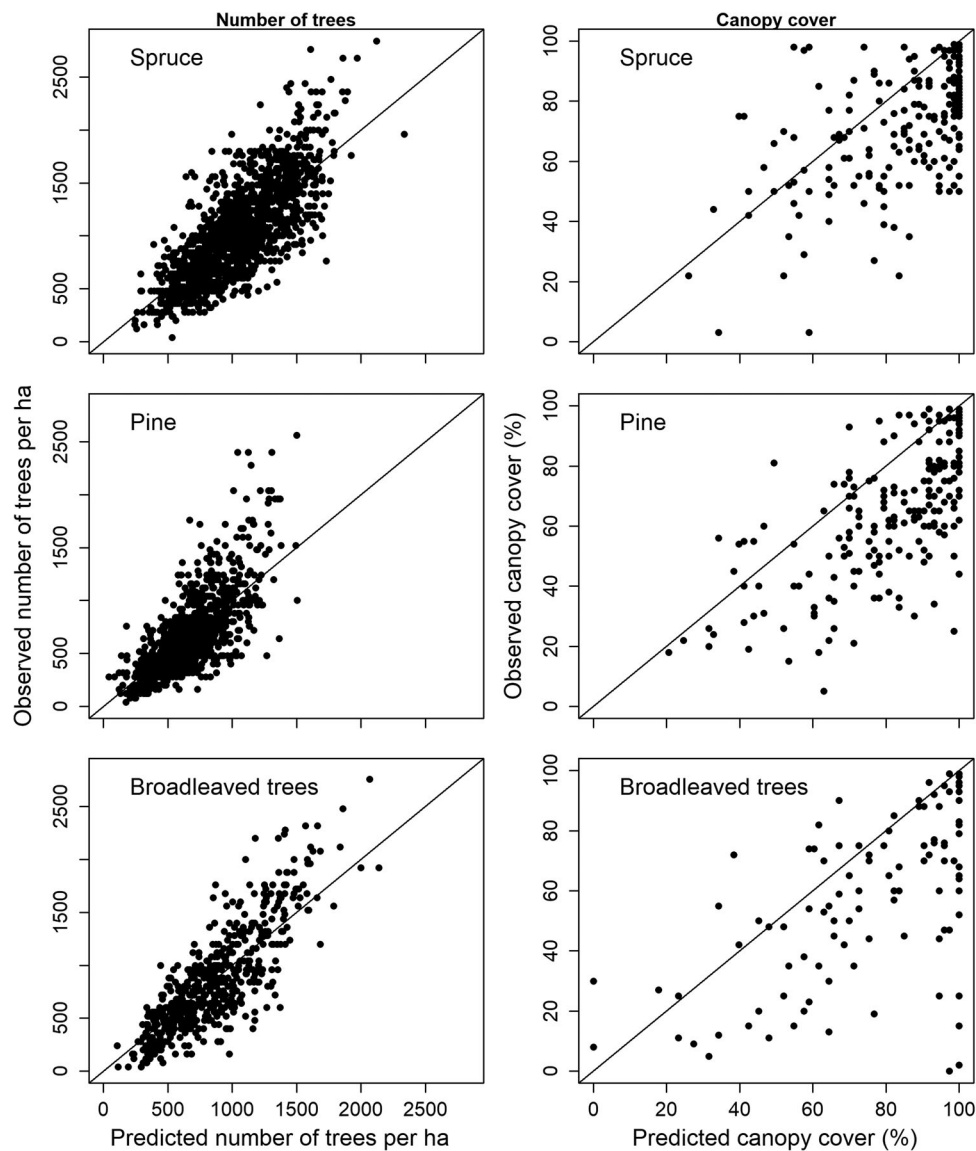


Figure 2. Observed vs. predicted stem density (number of trees per ha, left column), and canopy cover (right column) stratified into three tree species groups: spruce (top row), pine (middle row), and broadleaved trees (bottom row).

density. Similarly, also the other accuracy statistics PA, UA, and F1 score improved (Table 8). Only PA of class 3 decreased when using forest attributes in the model since more routes that were marked as class 3 in the reference were predicted as class 2.

Table 6. Characteristics of the fitted models and canopy cover relationship.

	Stem density	Canopy cover ^a
Overall		
RMSE _{cv}	300.9	23.3
RMSE _{cv} %	35.0	34.0
Norway spruce		
RMSE _{cv}	307.9	20.2
RMSE _{cv} %	29.9	30.8
Scots pine		
RMSE _{cv}	277.4	23.6
RMSE _{cv} %	42.5	36.2
Broadleaved trees		
RMSE _{cv}	330.7	28.7
RMSE _{cv} %	39.1	38.8

^aRMSE_{cv} in percentage points, RMSE_{cv}% in percentage to the mean.

Discussion

In this study, we modelled and mapped the forest attributes stem density and canopy cover respectively using NFI and remote-sensing data collected over a large area in Norway. We included these forest attribute maps as inputs in the spatially explicit avalanche terrain model AutoATES-Forest in order to improve terrain classification maps for recreational activities. Forest attribute and avalanche terrain maps may in this way become valuable tools for informing forest management decisions aiming at the utilization of forests as nature-based solutions for avalanche-related disaster risk reduction (EEA 2021).

We predicted stem density and found an overall R^2 and cross-validated RMSE of 0.62 and 301 (35%), respectively. Tompalski et al. (2019) found similar results with R^2 and RMSE of 0.37 and 293 (42%), respectively, for modelling stem density in Canada. Lindberg and Hollaus (2012) compared area-based and single tree-based approaches for estimating

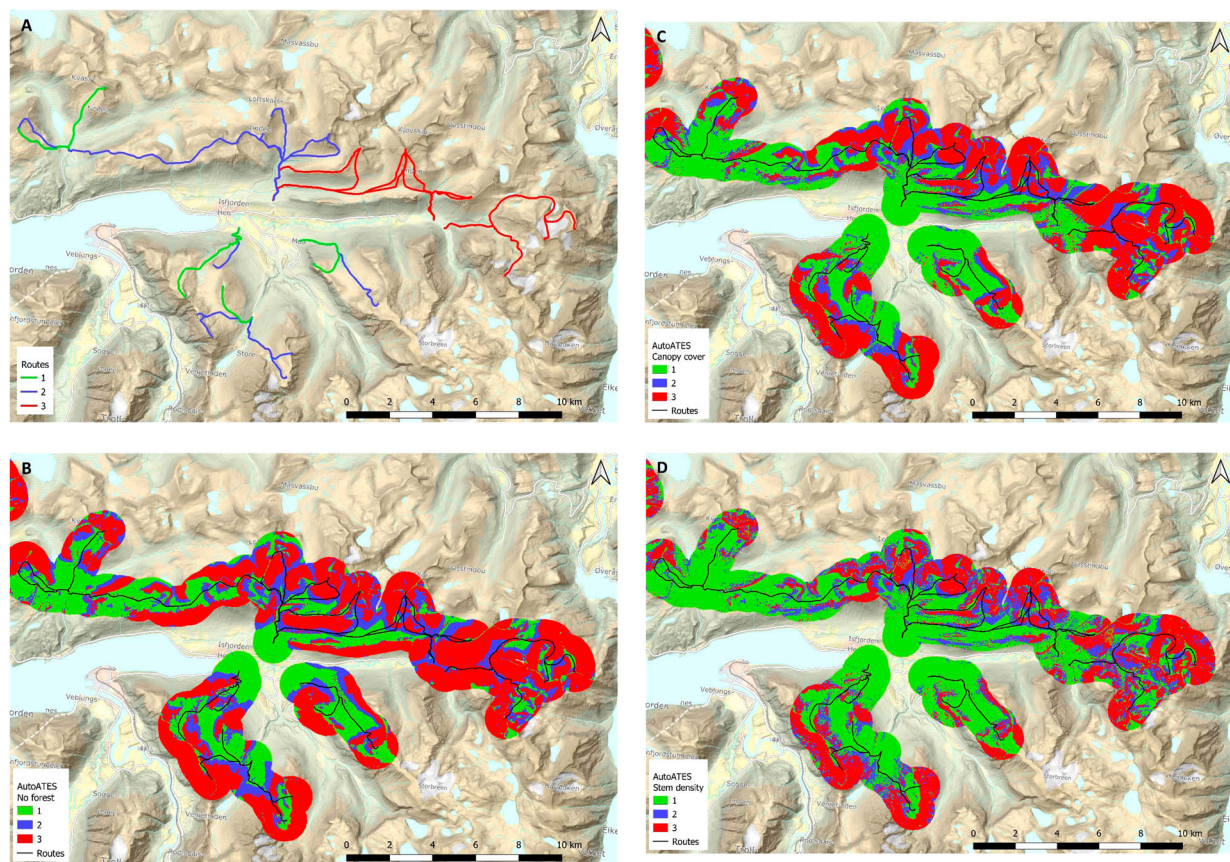


Figure 3. Area around the town Isforden; (A) manually ATES classification of touring routes according to the part with the greatest consequence used as reference (class 1 = simple in green, class 2 = challenging in blue, class 3 = complex in red); (B) output of AutoATES model without forest; (C) output of AutoATES-Forest model with forest canopy cover as model input; (D) output of AutoATES-Forest model with forest stem density as model input.

the number of trees and found RMSE of 53% (area-based) and 63–92% (single tree based). Ene et al. (2012) used the single tree-based approach and reported a 46–50% detection rate for stem number estimates in heterogeneous boreal forests. Eysn et al. (2015) reported 47% overall tree detection rate in heterogeneous alpine forest. Stem density is difficult to predict using the type of remote-sensing data used in this study. While using very high-resolution ALS or drone data (Puliti et al. 2020; Persson et al. 2022) would allow for analyses on a single tree trunk level that might result in higher

accuracies, collecting such high-resolution data on the large spatial scale used in this study is currently not feasible.

In an initial analysis, we also compared canopy cover calculated as proposed by Korhonen et al. (2011) with canopy cover from the NFI. However, this relationship was worse than our voxel-based approach and therefore not further considered in this study. The relation between predicted and observed canopy cover was not as good as for stem density. This can partially be attributed to the fact that canopy cover in the NFI is not measured, but visually assessed by the NFI crew.

Table 7. Confusion matrices for 282 km manually classified routes (ATES) in Romsdalen and the automated ATES algorithms AutoATES, AutoATES-Forest (canopy cover) and AutoATES-Forest (stem density) on entire-route level.

No forest parameters included		AutoATES		
Manually mapped (ATES)	Class 1 simple	Class 1	Class 2	Class 3
	Class 2 challenging	10.5 (3)	21.8 (7)	10.6 (2)
	Class 3 complex	0 (0)	59.9 (12)	71.2 (14)
Including canopy cover		AutoATES-Forest		
Manually mapped (ATES)	Class 1 simple	Class 1	Class 2	Class 3
	Class 2 challenging	23.1 (6)	13.8 (5)	6.0 (1)
	Class 3 complex	0 (0)	90.1 (16)	41.0 (10)
Including stem density		AutoATES-Forest		
Manually mapped (ATES)	Class 1 simple	Class 1	Class 2	Class 3
	Class 2 challenging	29.2 (8)	13.7 (4)	0 (0)
	Class 3 complex	24.7 (3)	78.9 (16)	27.5 (7)
		0 (0)	38.7 (5)	69.0 (9)

Notes: Routes were classified according to the 95th percentile of AutoATES and AutoATES-Forest predictions. Values represent km of routes (route count is given in parentheses).

Table 8. accuracies for routes assigned to one class; routes were assigned one predicted value using the 95th percentile of predicted pixel values within a route; OA = Overall accuracy, PA = Producer's accuracy, UA = User's accuracy.

	OA	F1 score			PA			UA		
		Class 1 simple	Class 2 challenging	Class 3 complex	Class 1 simple	Class 2 challenging	Class 3 complex	Class 1 simple	Class 2 challenging	Class 3 complex
AutoATES No forest	0.55	0.39	0.51	0.62	0.25	0.46	0.79	1.00	0.57	0.51
AutoATES Canopy cover	0.67	0.70	0.68	0.66	0.54	0.69	0.70	1.00	0.66	0.62
AutoATES Stem density	0.63	0.60	0.60	0.68	0.68	0.60	0.64	0.54	0.60	0.72

Using the forest attributes stem density or canopy cover in the AutoATES-Forest models improved the route classification compared to the AutoATES model without forest attributes. Especially the percentage of class 1 (simple) routes that wrongly were classified as class 2 (challenging) or 3 (complex) was reduced. This can partly be explained by the fact that forest is defined explicitly for class 1 terrain in the public communication model (Table 2) and the technical model of ATES. Forest is a distinctive terrain characteristic for class 1, while class 2 usually has sparser forest, and class 3 is typically non-forested. However, the forest characteristic is not a defining parameter. This means that non-forested terrain could be class 1, and forested area could be class 3 if other terrain characteristics are given considerable weight.

When classifying ski-touring routes using manual ATES, the overall class is decided by the most hazardous area on a given route. This means that if the route is located mostly in simple terrain (class 1), the whole route could be classified as complex terrain (class 3) if there is a short section of this type of terrain along the given route. This is a deliberate design feature that errs on the side of safety. A result of this is that even though the algorithm, which works on the pixel level, defines a large percentage of a given route as less hazardous than the manual classification class rating, it is not wrong. Therefore, the 95th percentile of pixel values from the AutoATES terrain classification was used for assigning one terrain class to a route.

Using the forest attribute canopy cover resulted in slightly better classifications, but the difference between the two forest metrics was not as great as the difference between the use of forest metrics and the lack of forest metrics. These results indicate that adding spatially explicit information on forest attributes are beneficial for terrain evaluation. Other forest properties such as diameter distributions can be mapped from ALS data (Räty et al. 2021) and should be considered as input to avalanche terrain models in the future. Furthermore, avalanche terrain models could be further improved to utilize forest attributes as continuous values.

Brožová et al. (2020) evaluated variables extracted from ALS and photogrammetric point clouds towards their influence on simulation results of avalanche runout in a case study in Switzerland. Remotely sensed tree heights, canopy coverage, and DTM roughness were used for avalanche simulation. They concluded that remote-sensing data with a fine resolution of about 1 m × 1 m were generally suitable to model relevant forest attributes used as input for avalanche simulation. The simulation results using the two data sources – ALS and photogrammetric point clouds – were both sufficiently accurate for numerical modelling and for real-world applications in snow avalanche hazard mapping using the RAMMS model. However, simulations of only two avalanches were analysed. Bühler et al. (2022) described automated avalanche runout mapping using the RAMMS model in one Canton in Switzerland. Terrain slope and the forest properties percentage of crown cover and gap width were used to predict a “protection forest index” for each forested raster cell of 5 m × 5 m. Threshold values were found defining a sufficient protection forest index for two different return period scenarios (frequent and rare). This way, forest was treated as a binary input variable

either being present and influencing an avalanche or not. This approach is similar to ours for the runout zone where we define four groups of forest types that influence avalanche behaviour. However, Bühler et al. (2022) focus on avalanche hazard modelling for regional land use planning with avalanche return periods of 10–30 and 100–300 years. In the present study, we focus on avalanche terrain modelling for backcountry skiing, where return periods are much shorter.

A wider implication of these findings is that the value of ecosystem services, such as the protection function of forests, is often difficult to assess. In this respect, our study showed the positive effect of forest in avalanche terrain modelling, and this is something that can be quantified, at least spatially. The authors jointly consider that no price should be put on human lives and therefore we will not enter into discussion of the monetary value of such protection here, though examples exist (e.g. Grilli et al. 2020) and it is no doubt an important subject for forest owners whose primary interests are timber revenues. In this respect, however, we feel that protection should influence forest management decisions, but that significantly more research is required to investigate optimal forest management of protective forests in a Norwegian context.

Finally, mapping the probability of avalanche releases is meant as an additional planning aid for route choice, much like a weather forecast, and can be wrong. Avalanche conditions change dramatically depending on snow conditions and these are not in any way included in the ATES system. While we strive to improve the decision-making tools, these are no substitute for local evaluation of the current conditions on the ground, and this requires specific training and experience. Even then, avalanches pose a significant threat and safety is solely the responsibility of the individual. Nonetheless, we can conclude that the inclusion of forest attributes in avalanche terrain models can considerably improve their predictive performance.

Acknowledgements

We would like to thank two unknown reviewers for constructive comments that considerably improved our manuscript.

Disclosure statement

No potential conflict of interest was reported by the author(s).

ORCID

Johannes Schumacher  <http://orcid.org/0000-0003-4592-9035>

Håvard Toft  <http://orcid.org/0000-0003-1748-6329>

Marius Hauglin  <http://orcid.org/0000-0003-2230-1288>

Rasmus Astrup  <http://orcid.org/0000-0003-2988-9520>

Johannes Breidenbach  <http://orcid.org/0000-0002-3137-7236>

References

- Astrup R, Rahlf J, Bjørkelo K, Debella-Gilo M, Gjertsen A-K, Breidenbach J. 2019. Forest information at multiple scales: development, evaluation and application of the Norwegian forest resources map SR16. *Scand J For Res.* 34(6):484–496. doi:10.1080/02827581.2019.1588989.
- Barbolini M, Pagliardi M, Ferro F, Corradeghini P. 2011. Avalanche hazard mapping over large undocumented areas. *Nat Hazards.* 56:451–464. doi:10.1007/s11069-009-9434-8.
- Bebi P, Kienast F, Schönenberger W. 2001. Assessing structures in mountain forests as a basis for investigating the forests' dynamics and protective function. *For Ecol Manage.* 145:3–14. doi:10.1016/S0378-1127(00)00570-3.
- Brang P, Schönenberger W, Frehner M, Schwitter R, Thormann JJ, Wasser B. 2006. Management of protection forests in the European Alps: an overview. *For Snow Landsc Res.* 80(1):23–44.
- Breidenbach J, Granhus A, Høyen G, Eriksen R, Astrup R. 2020a. A century of national forest inventory in Norway – informing past, present, and future decisions. *For Ecosyst.* 7(46): 1–19. doi:10.1186/s40663-020-00261-0.
- Breidenbach J, Waser LT, Debella-Gilo M, Schumacher J, Rahlf J, Hauglin M, Puliti S, Astrup R. 2020b. National mapping and estimation of forest area by dominant tree species using Sentinel-2 data. *Can J For Res.* 51(3):365–379.
- Broszofski KD, Froese RE, Falkowski MJ, Banskota A. 2014. A review of methods for mapping and prediction of inventory attributes for operational forest management. *For Sci.* 60:733–756.
- Brožová N, Fischer JT, Bühler Y, Bartelt P, Bebi P. 2020. Determining forest parameters for avalanche simulation using remote sensing data. *Cold Reg Sci Technol.* 172:102976. doi:10.1016/j.coldregions.2019.102976.
- Bühler Y, Bebi P, Christen M, Margreth S, Stoffel L, Stoffel A, Marty C, Schmucki G, Caviezel A, Kühne R, et al. 2022. Automated avalanche hazard indication mapping on state wide scale. *Nat Hazards Earth Syst Sci Discuss.* 2022:1–22. doi:10.5194/nhess-2022-11.
- Campbell C, Gould B. 2013. A proposed practical model for zoning with the scale. *International Snow Science Workshop; Grenoble – Chamonix Mont-Blanc.*
- Congalton RG, Green K. 2008. Assessing the accuracy of remotely sensed data: principles and practices. 2nd ed. Boca Raton: CRC Press.
- D'Amboise CJL, Neuhauser M, Teich M, Huber A, Kofler A, Perzl F, Fromm R, Kleemayr K, Fischer J-T. 2021. Flow-Py v1.0: a customizable, open-source simulation tool to estimate runout and intensity of gravitational mass flows. *Geosci Model Dev Discuss.* 2021:1–28. doi:10.5194/gmd-2021-277.
- Delparte DM. 2008. Avalanche terrain modeling in Glacier National Park, Canada. Calgary: University of Calgary (Canada).
- Drusch M, Del Bello U, Carlier S, Colin O, Fernandez V, Gascon F, Hoersch B, Isola C, Laberinti P, Martimort P, et al. 2012. Sentinel-2: ESA's optical high-resolution mission for GMES operational services. *Remote Sens Environ.* 120:25–36. doi:10.1016/j.rse.2011.11.026.
- EEA. 2021. Nature-based solutions in Europe: policy, knowledge and practice for climate change adaptation and disaster risk reduction. Copenhagen: Publications Office of the European Union.
- Ene L, Næsset E, Gobakken T. 2012. Single tree detection in heterogeneous boreal forests using airborne laser scanning and area-based stem number estimates. *Int J Remote Sens.* 33:5171–5193. doi:10.1080/01431161.2012.657363.
- Eysn L, Hollaus M, Lindberg E, Berger F, Monnet J-M, Dalponte M, Kobal M, Pellegrini M, Lingua E, Mongus D, Pfeifer N. 2015. A benchmark of lidar-based single tree detection methods using heterogeneous forest data from the Alpine Space. *Forests.* 6:1721–1747. doi:10.3390/f6051721.
- Grilli G, Fratini R, Marone E, Sacchelli S. 2020. A spatial-based tool for the analysis of payments for forest ecosystem services related to hydro-geological protection. *For Policy Econ.* 111:102039. doi:10.1016/j.forpol.2019.102039.
- Harvey S, Schmudlach G, Bühler Y, Dürr L, Stoffel A, Christen M. 2018. Avalanche terrain maps for backcountry skiing in Switzerland. *International Snow Science Workshop Proceedings; Innsbruck, Austria.* p 1625–1631.
- Hauglin M, Rahlf J, Schumacher J, Astrup R, Breidenbach J. 2021. Large scale mapping of forest attributes using heterogeneous sets of airborne laser scanning and national forest inventory data. *For Ecosyst.* 8:65. doi:10.1186/s40663-021-00338-4.
- Jang JSR, Sun CT, Mizutani E. 1997. Neuro-fuzzy and soft computing: a computational approach to learning and machine intelligence. *IEEE Trans Automat Contr.* 42:1482–1484.

- Kartverket. 2019. Høydedata og terrengmodeller for landområdene. [accessed 2020 Mar 11]. <https://www.kartverket.no/data/Hoydedata-og-terrengmodeller/>.
- Korhonen L, Korpela I, Heiskanen J, Maltamo M. 2011. Airborne discrete-return LIDAR data in the estimation of vertical canopy cover, angular canopy closure and leaf area index. *Remote Sens Environ.* 115:1065–1080. doi:10.1016/j.rse.2010.12.011.
- Larsen HT, Hendriks J, Schauer A, Langford R, Statham L, Campbell C, Neuhauser M, Fischer J-T, Sykes J. 2020a. Development of automated avalanche terrain exposure scale maps: current and future. *Virtual Snow Science Workshop* 2020.
- Larsen HT, Hendriks J, Slåtten MS, Engeset RV. 2020b. Developing nationwide avalanche terrain maps for Norway. *Nat Hazards.* 103:2829–2847. doi:10.1007/s11069-020-04104-7.
- Lindberg E, Hollaus M. 2012. Comparison of methods for estimation of stem volume, stem number and Basal area from airborne laser scanning data in a hemi-boreal forest. *Remote Sens.* 4:1004–1023. doi:10.3390/rs4041004.
- Lindberg E, Holmgren J, Olofsson K, Wallerman J, Olsson H. 2010. Estimation of tree lists from airborne laser scanning by combining single-tree and area-based methods. *Int J Remote Sens.* 31:1175–1192. doi:10.1080/01431160903380649.
- NGI. 2022. Snøskredulykker med død. *Norwegian Geotech. Inst.* <https://www.ngi.no/Tjenester/Fagekspertise/Snoeskred/snoskred.no2/Snoeskredulykker-med-doed>.
- NIBIO. 2022. Kilden. [accessed 2022 Feb 15]. https://kilden.nibio.no/?topic=skogportal&lang=nb&X=6815209.58&Y=209562.35&zoom=2.3333333333333333&bgLayer=graatone_cache&layers_opacity=0.75&layers=skogressurs_volum_r.
- Næsset E. 2002. Predicting forest stand characteristics with airborne scanning laser using a practical two-stage procedure and field data. *Remote Sens Environ.* 80:88–99. doi:10.1016/S0034-4257(01)00290-5.
- Næsset E, Bjerknes K-O. 2001. Estimating tree heights and number of stems in young forest stands using airborne laser scanner data. *Remote Sens Environ.* 78:328–340. doi:10.1016/S0034-4257(01)00228-0.
- Persson HJ, Olofsson K, Holmgren J. 2022. Two-phase forest inventory using very-high-resolution laser scanning. *Remote Sens Environ.* 271:112909. doi:10.1016/j.rse.2022.112909.
- Pinheiro J, Bates D, DebRoy S, Sarkar D, EISPAC authors, Heisterkamp S, Van Willigen B, Ranke J, R Core Team. 2020. nlme: linear and nonlinear mixed effects models.
- Puliti S, Breidenbach J, Astrup R. 2020. Estimation of forest growing stock volume with UAV laser scanning data: can it be done without field data? *Remote Sens.* 12(1245):1–19. doi:10.3390/rs12081245.
- Räty J, Astrup R, Breidenbach J. 2021. Prediction and model-assisted estimation of diameter distributions using Norwegian national forest inventory and airborne laser scanning data. *Can J For Res.* 51:1521–1533. doi:10.1139/cjfr-2020-0440.
- R Core Team. 2020. R: a language and environment for statistical computing.
- Schmudlach G, Köhler J. 2016. Automated avalanche risk rating of back-country ski routes. *International Snow Science Workshop Proceedings; Breckenridge, Colorado, USA.* p 450–456.
- Sharp E, Haegeli P, Welch M. 2018. Patterns in the exposure of ski guides to avalanche terrain. *International Snow Science Workshop; Oct 7–12; Innsbruck, Austria.*
- Statham G, McMahon B, Tomm I. 2006. The avalanche terrain exposure scale. *Proceedings of the International Snow Science Workshop; Telluride, CO, USA.* p. 491–497.
- Teich M, Bartelt P, Grêt-Regamey A, Bebi P. 2012. Snow avalanches in forested terrain: influence of forest parameters, topography, and avalanche characteristics on runout distance. *Artic Antarct Alp Res.* 44:509–519. doi:10.1657/1938-4246-44.4.509.
- Teich M, Fischer J-T, Feistl T, Bebi P, Christen M, Grêt-Regamey A. 2014. Computational snow avalanche simulation in forested terrain. *Nat Hazards Earth Syst Sci.* 14:2233–2248. doi:10.5194/nhess-14-2233-2014.
- Tompalski P, White JC, Coops NC, Wulder MA. 2019. Quantifying the contribution of spectral metrics derived from digital aerial photogrammetry to area-based models of forest inventory attributes. *Remote Sens Environ.* 234:111434. doi:10.1016/J.RSE.2019.111434.
- Varsom. 2022. Dødsfall og skader fra snøskred og på islagte vann. <https://varsom.no/ulykker/snoskredulykker-og-hendelser/>.
- Veitinger J, Purves RS, Sovilla B. 2016. Potential slab avalanche release area identification from estimated winter terrain: a multi-scale, fuzzy logic approach. *Nat Hazards Earth Syst Sci.* 16:2211–2225. doi:10.5194/nhess-16-2211-2016.
- Venables WN, Ripley BD. 2002. *Modern applied statistics with S.* 4th ed. New York: Springer.
- Viken KO. 2021. Landsskogtakseringens feltinstruks – 2021, NIBIO-bok; NIBIO.

Appendix

Table A1. stem density models; coefficients, their standard errors, and *p*-values for the tree species-specific linear regression models for spruce, pine, and broadleaved trees.

Variable	Estimate	Std. error	<i>p</i> -Value
Stem density model for spruce			
Intercept	−73.85	130.87	.573
h75f	37.52	23.48	.110
h75fsq	−1.37	0.65	.034
pctab2f	−175.99	406.92	.665
pctab2fsq	1862.63	421.25	<.001
d6f	1122.08	103.12	<.001
NDVI	414.73	113.61	<.001
slope	−1.94	0.57	<.001
h75f × pctab2f	−89.52	35	.011
h75fsq × pctab2fsq	1.57	0.74	.033
Stem density model for pine			
Intercept	−171.32	109.02	.116
h75f	16.39	15.27	.283
h75fsq	0.60	0.65	.361
pctab2f	364.46	421.98	.388
pctab2fsq	1491.58	375.16	<.001
d4f	986.33	140.30	<.001
NDVI	240.69	110.80	.03
Slope	−1.84	0.54	.001
h75f × pctab2f	−126.86	32.79	<.001
h75fsq × pctab2fsq	2.37	0.84	.005
Stem density model for broadleaved trees			
Intercept	191.58	41.93	<.001
h75fsq	−2.07	0.25	<.001
pctab2fsq	1255.46	91.02	<.001
d6f	993.70	180.47	<.001

Table A2. Variance components for fixed and random effects and residual of the stem density models for spruce, pine, and broadleaved forest.

	Variance (%)
Norway spruce	
Fixed effects	50.91
Random effect	5.59
Residual	43.50
Scots pine	
Fixed effects	40.72
Random effect	10.81
Residual	48.47
Broadleaved trees	
Fixed effects	48.08
Random effect	13.99
Residual	37.93